Intraepithelial Vagal Sensory Nerve Terminals in Rat Pulmonary Neuroepithelial Bodies Express $P2X_3$ Receptors

Inge Brouns, Dirk Adriaensen, Geoff Burnstock, and Jean-Pierre Timmermans

Laboratory of Cell Biology and Histology, University of Antwerp, Antwerp, Belgium; and Autonomic Neuroscience Institute, Royal Free Hospital School of Medicine, London, United Kingdom

The neurotransmitters/modulators involved in the interaction between pulmonary neuroepithelial bodies (NEBs) and the vagal sensory component of their innervation have not yet been elucidated. Because $P2X_3$ purinoreceptors are known to be strongly expressed in peripheral sensory neurons, the aim of the present study was to examine the localization of nerve endings expressing $P2X_3$ purinoreceptors in the rat lung in general and those contacting pulmonary NEBs in particular. Most striking were intraepithelial arborizations of $P2X_3$ purinoceptor–immunoreactive (IR) nerve terminals, which in all cases appeared to ramify between calcitonin gene–related peptide (CGRP)– or calbindin D28k (CB)–labeled NEB cells. However, not all NEBs received nerve endings expressing $P2X_3$ receptors. Using CGRP and CB staining as markers for two different sensory components of the innervation of NEBs, it was revealed that $P2X_3$ receptor and CB immunoreactivity were colocalized, whereas CGRP-IR fibers clearly formed a different population. The disappearance of characteristic $P2X_3$ receptor–positive nerve fibers in contact with NEBs after infranodosal vagal crush and colocalization of tracer and $P2X_3$ receptor immunoreactivity in vagal nodose neuronal cell bodies in retrograde tracing experiments further supports our hypothesis that the $P2X_3$ receptor–IR nerve fibers contacting NEBs have their origin in the vagal sensory nodose ganglia. Combination of quinacrine accumulation in NEBs, suggestive of the presence of high concentrations of adenosine triphosphate (ATP) in their secretory vesicles, and $P2X_3$ receptor staining showed that the branching intraepithelial $P2X_3$ receptor-IR nerve terminals in rat lungs were exclusively associated with quinacrine-stained NEBs. We conclude that ATP might act as a neurotransmitter/neuromodulator in the vagal sensory innervation of NEBs via a $P2X_3$ receptor–mediated pathway. Further studies are necessary to determine whether the $P2X_3$ receptor–expressing neurons, specifically innervating NEBs in the rat lung, belong to a population of $P2X_3$ receptor–IR nociceptive vagal nodose neurons.

Pulmonary neuroepithelial bodies (NEBs) are extensively innervated, organoid groups of neuroendocrine cells present in the epithelial lining of the airways of all air-breathing vertebrates investigated so far (for review, *see* References 1–3). NEBs are considered to play a major role in the local regulation of airway function in health and disease, in view of their characteristic location, receptor-effector–like morphology, and complex innervation pattern, and because they contain many bioactive substances. It has been shown that NEBs are capable of responding to hypoxia (4–6) in an innervation-dependent way, but many other functional hypotheses have been put forward (for review, *see* Reference 7).

The complex innervation pattern of pulmonary NEBs appears to consist of afferent and efferent components (2, 3). It has been revealed by tracer experiments that the vagal sensory component of the innervation of rat NEBs originates in the nodose ganglia (8, 9). At present, it is still unknown which neurotransmitters/neuromodulators might be involved in the interaction between vagal sensory fibers and NEBs. Recently, quinacrine accumulation was demonstrated in the neuroendocrine cells of rat pulmonary NEBs (10), which indicates the presence of high levels of adenosine triphosphate (ATP), bound to peptides in secretory vesicles (11–14). It therefore appeared interesting to investigate the possibility that ATP might be involved in the vagal nodose neurotransmission in rat pulmonary NEBs. The presence of ATP receptors may be considered crucial for such a direct involvement of ATP.

Two major families of ATP receptors (purinergic receptors, purinoceptors) have been identified as P1 and P2, showing different affinities to adenosine and ATP/adenosine diphosphate, respectively (15, 16). The P2 receptors fall into two families, P2X and P2Y, the former of which are ligand-gated ion channels, the latter G protein–coupled receptors (17, 18). Currently, seven members of the P2X family have been identified (19), and most of these receptors are widely distributed not only throughout the central and peripheral nervous system, but also in non-neuronal tissues (20, 21). The $P2X_3$ purinoceptor, one of the receptor subtypes, however, appears to be limited largely to peripheral sensory neurons. This receptor was cloned, characterized, and shown by *in situ* hybridization to be located in small nociceptive sensory neurons (22, 23). These findings were later confirmed and extended by using immunohistochemical methods (24–29). There is a growing body of evidence that ATP can activate peripheral nociceptors (29–31). Several reports suggest that the nociceptive actions of ATP are mediated at least partly by interactions with $P2X_3$ receptors. Rat tooth-pulp afferents, which are believed to be nociceptive, were shown to express $P2X_3$ receptor immunoreactivity and to respond to purinoceptor ligands with a pharmacologic profile indicative of $P2X_3$ receptor activation (25). Low-threshold mechanoreceptive afferents, on the other hand, did not show these properties (25). The restricted distribution of $P2X_3$ receptors, possibly forming heteromultimers with the $P2X_2$ receptors, suggests that this receptor subtype plays an important role in endowing nociceptors with a sensitivity to ATP (23). Because the $P2X_3$ receptor has been demonstrated on small-

(*Received in original form September 14, 1999 and in revised form February 27, 2000*)

Address correspondence to: Prof. Dr. Jean-Pierre Timmermans, Laboratory for Cell Biology & Histology, University of Antwerp, Groenenborgerlaan 171, B-2020 Antwerp, Belgium. E-mail: jptimmer@ruca.ua.ac.be

Abbreviations: adenosine triphosphate, ATP; calbindin D28k, CB; calcitonin gene-related peptide, CGRP; dorsal root ganglia, DRG; fluorescein isothiocyanate, FITC; immunoreactive, IR; neuroepithelial body, NEB; normal horse serum, NHS; overnight, ON; primary antiserum diluent, PAD; phosphate-buffered saline, PBS; room temperature, RT; tyramide signal amplification, TSA.

Am. J. Respir. Cell Mol. Biol. Vol. 23, pp. 52–61, 2000
Internet address: www.atsjournals.org

or medium-sized neurons in the vagal nodose ganglia in rat and monkey (24, 25, 32), it might be a candidate to mediate purinergic signaling in rat NEBs.

The aim of this study was to examine the localization of $P2X_3$ receptor–immunoreactive (IR) nerve endings in the rat lung in general and in relation to pulmonary NEBs in particular. To this end, immunocytochemical staining using $P2X_3$ receptor antibodies (29, 33) and subsequent labeling with antibodies to known markers for rat NEBs were applied. A combination of quinacrine accumulation in NEBs and $P2X_3$ receptor immunolabeling was used to reveal possible functional units. Nerve lesion and retrograde tracing experiments were carried out to investigate the involvement of vagal nodose afferents.

Materials and Methods

Animals

In this study, Wistar rats ($n = 14$; Iffa Credo, Brussels, Belgium) were used. All animals were kept in acrylic cages with wood shavings in a climatized room (12/12 h light/dark cycle; 22 ± 3°C) and provided with water and food *ad libitum*. National and international principles of laboratory animal care were followed and the experiments were approved by the local ethics committee of the University of Antwerp.

$P2X_3$ Receptor Localization

Tissue processing. The animals (adults, $n = 2$; 4 to 5 wk old, $n = 4$) were killed by an overdose of Nembutal (sodium pentobarbital). Lungs were intratracheally instilled with 4% phosphate-buffered paraformaldehyde, dissected, degassed, and fixed for an additional 2 h. The tissues were rinsed in phosphate-buffered saline (PBS) (0.01 M, pH 7.4), stored overnight (ON) in 20% sucrose (in PBS; 4°C), and mounted in Tissue Tek (Sakura Finetek Europe, Zoeterwoude, The Netherlands) on a cryostat chuck by freezing in a CO_2 chamber. Cryostat sections, 20-μm thick, were thaw-mounted on poly-L-lysine–coated microscope slides, air-dried, and stored at −80°C in a closed container.

Immunocytochemistry. Freeze-sections were allowed to warm to room temperature (RT) in a closed container, and endogenous peroxidase activity was blocked by H_2O_2 (0.4% in 50% methanol; 10 min). The sections were rinsed in PBS, preincubated (30 min) with the same solution to be used for dilution of the primary antibody (10% normal horse serum [NHS], 0.05% thimerosal; in PBS), and incubated (ON; RT) with a rabbit polyclonal antibody to $P2X_3$ receptors (gift from Roche Bioscience, Palo Alto, CA; dilution 0.625 μg/ml for amplified and 0.625 or 10 μg/ml for nonamplified immunostaining; *see* Reference 33), followed by incubation with a biotinylated donkey antirabbit antibody (diluted 1:500 in a solution containing 1% NHS, 0.05% thimerosal; in PBS; 1 h; RT; Jackson, West Grove, PA), and Extr-Avidin-horseradish peroxidase (1:1,500 in PBS containing 0.05% thimerosal; 1 h; RT; Sigma, Bornem, Belgium). To allow for an enhanced staining of $P2X_3$ purinoceptors on nerve fiber endings, an indirect tyramide signal amplification (TSA) (TSA kit; NEN, Boston, MA) was applied. Between subsequent steps the sections were washed (0.05% Tween 20 in PBS; three times for 5 min each; RT). Sections were incubated with biotinyl tyramide in "amplification solution" (1:50; 8 min; RT). Visualization was performed using a fluorescein isothiocyanate (FITC)–conjugated streptavidin (diluted 1:200 in PBS containing 0.05% thimerosal; 10 min; Amersham, Roosendaal, The Netherlands) after TSA or, for control purposes, directly after the incubation with the biotinylated donkey antirabbit antibody. The sections were mounted in Vectashield (Vector Laboratories, Burlingame, CA).

Immunocytochemical Double Staining of $P2X_3$ Receptors and Neuroepithelial Bodies

For the simultaneous demonstration of $P2X_3$ receptor–IR nerve fibers and pulmonary NEBs, lung sections that were processed for $P2X_3$ receptor staining were additionally subjected to an indirect immunocytochemical staining using rabbit polyclonal antibodies to calcitonin gene-related peptide (CGRP) (diluted 1:200 in primary antiserum diluent [PAD]: PBS containing 10% normal goat serum, 0.1% bovine serum albumin, 0.05% thimerosal, and 0.01% NaN_3; ON; RT; Affinity, Exeter, UK) or calbindin D28k (CB) (1:2,500 in PAD; ON; RT; SWant, Bellinzona, Switzerland), and a Cy-3–conjugated goat antirabbit (GAR) serum (GAR–Cy-3; 1:200 in PAD; 1 h; RT; Jackson). PBS was used as a rinsing solution, and the sections were mounted in Vectashield. The use of TSA allowed a consecutive immunostaining with two rabbit antisera, as previously described (34).

Fourteen random lung sections from each animal processed for the localization of $P2X_3$ receptors and NEBs ($n = 6$) were used for quantitative analysis. The total numbers of NEBs (marked by their CGRP or CB staining), $P2X_3$ receptor–IR intraepithelial nerve terminals, and NEBs receiving $P2X_3$ receptor–IR innervation were counted.

Quinacrine Accumulation in Neuroepithelial Bodies and Consecutive Demonstration of $P2X_3$ Receptor–IR Innervation

Wistar rats (4 to 5 wk old; $n = 3$) were pretreated for quinacrine accumulation (10, 35). To this end, the animals were injected intraperitoneally with 50 mg/kg body weight quinacrine (Mepacrine; Sigma; dissolved in injectable water) 24 h before death. The animals were killed by an overdose of Nembutal. The lungs were isolated and freshly frozen on a cryostat chuck in a CO_2 chamber. Cryostat sections, 10 to 15 μm thick, were cut, collected on poly-L-lysine–coated glass slides, and instantly fixed on the slide using 4% phosphate-buffered paraformaldehyde (2 min). The sections were rinsed briefly in PBS and mounted in Vectashield. Quinacrine fluorescence was viewed and photographed immediately because of the rapid loss of fluorescence.

To verify whether quinacrine-storing NEBs are innervated by nerve fibers expressing $P2X_3$ purinoceptors, the distribution of quinacrine-positive pulmonary NEBs and $P2X_3$ receptor–labeled nerve fibers was compared. For this purpose, coverslips were removed from sections that had shown quinacrine-stained NEBs. After rinsing with PBS, the sections were air-dried and stored at −80°C until further treated for the immunofluorescent detection of $P2X_3$ receptors as described earlier.

$P2X_3$ Receptor–IR Innervation of Neuroepithelial Bodies after Unilateral Vagal Crush

Adult Wistar rats ($n = 3$) that had been deprived of food overnight were anesthetized by intramuscular injection of Hypnorm (1 ml/kg; fentanyl 0.315 mg/ml plus fluanisone 10 mg/ml; Janssen Pharmaceuticals, Beerse, Belgium) approximately 20 min after an intramuscular injection of atropine (0.2 mg/kg). When the animals were fully irresponsive, the left cervical vagal nerve was exposed about 15 mm caudal from the larynx by a ventral approach. The vagal nerve was crushed by smooth-surfaced tweezers for at least 15 s. At completion of the surgical procedure the skin was sutured. The animals were killed 3, 7, and 14 d after the surgical procedure, respectively, by an overdose of Nembutal, and the tissues were further processed for immunocytochemistry as described earlier.

$P2X_3$ Receptor Expression in Vagal Nodose Neurons Retrogradely Traced from the Lungs

Combined retrograde neuronal tracing (36) and immunocytochemistry were used to check whether vagal nodose neurons, specifically involved in pulmonary innervation, express $P2X_3$ receptors.

Adult Wistar rats ($n = 2$) were anesthetized by an intramuscular injection of Hypnorm (1 ml/kg). When the animals were fully irresponsive, the cervical trachea was exposed and an incision was made between two cartilage rings, allowing instillation of the yellow-fluorescent neuronal tracer Fluorogold (0.25 mg/ml in injectable water; 0.1 ml/kg; Fluorochrome, Englewood, CO) (37) in the lungs by means of a 1-ml syringe, connected to a polyethylene tube (1-mm diameter) that was inserted as far as the tracheal bifurcation. At 1 wk after instillation, the animals were killed by an overdose of Nembutal. Nodose ganglia were fixed in 4% paraformaldehyde (in PBS) and processed for immunocytochemistry as described for lung tissue.

In one of the rats, the right cervical vagal nerve was exposed and sectioned, and a portion of about 5-mm length was removed before the instillation of tracer.

Control Experiments

For $P2X_3$ receptor expression, negative staining controls were performed by substitution of nonimmune sera for the primary or secondary antisera and by preabsorption of the primary $P2X_3$ receptor antiserum with the receptor antigen (0.5 μl antibody was incubated with 24 μl peptide in 475 μl 10% NHS in 0.1 M PBS; ON).

As a positive control, cryostat sections of rat nodose ganglia, which are known to contain $P2X_3$ receptor–IR neurons (24, 25, 32), were processed for $P2X_3$ receptor immunostaining together with lung sections, as described earlier. Additional sections of nodose ganglia were immunostained without TSA enhancement.

To check for non–cross-reactivity after consecutive double staining with two rabbit primary antisera, the results of single immunostaining for both substances were evaluated and compared with those from double labeling. Staining controls were performed by omission of the primary antiserum of the second incubation. Also, a nonamplified staining with antibodies to $P2X_3$ receptors, using the same concentration (0.625 μg/ml) as for the TSA-enhanced reaction, was routinely included.

In the unilateral vagal crush experiments, lungs contralateral to the denervated side were regarded as control lungs with respect to the vagal sensory component of the NEB innervation (8).

Vagal nodose ganglia of the denervated side of rats that underwent a unilateral vagotomy before the intraluminal instillation of Fluorogold in the lungs were used as controls for the specific vagal transport of the tracer to nodose neurons.

Microscopic Analysis

An epifluorescence microscope (Zeiss Axiophot) equipped with filters for the visualization of FITC (Zeiss 17; BP 485-20/ FT 510/ BP 515-565), Cy-3 (Zeiss 14; LP 510-KP 560/ FT 580/ LP 590), and quinacrine (Zeiss 5; BP 395-440/ FT 460/ LP 470), was used to evaluate the results.

To obtain detailed images of the individual nerve endings in NEBs, a confocal laser scanning microscope (Zeiss LSM 410) and the attached image reconstruction facilities (Imaris 2.7 software; Fairfield Imaging, Kent, UK; Silicon Graphics Indigo 2 workstation) were used. A helium-neon laser (543 nm) and an argon laser (488 nm) were utilized for the excitation of Cy-3 and FITC, respectively.

Results

$P2X_3$ Receptor Immunoreactivity in the Lower Respiratory Tract of Rats

Nerve fibers containing $P2X_3$ receptor immunoreactivity were seen in sections of the vagal nerve at the level of the cervical trachea and in adventitial and submucosal nerve bundles of primary and intrapulmonary bronchi. Solitary nerve fibers or small bundles expressing $P2X_3$ receptor immunoreactivity were present, seen in the submucosa and in the lamina propria of bronchi and bronchioles. Nerve-fiber bundles harboring $P2X_3$ receptor–expressing fibers were also observed in the walls of terminal airways and in the interstitium of peripheral alveolar areas.

Most conspicuous were the terminal arborizations of $P2X_3$ receptor–positive nerve fibers at distinct locations in the epithelial layer of bronchi (Figure 1), bronchioles (Figure 2), terminal and respiratory bronchioles (Figure 3), and alveolar areas (Figures 4 and 5). These $P2X_3$ receptor–IR nerve fibers characteristically ramified at the base of the epithelium, giving rise to intraepithelial complexes. Some $P2X_3$ receptor–IR nerve fibers were seen to supply several intraepithelial complexes (Figure 2), whereas in other cases multiple nerve fibers terminated in just one complex (Figures 1b and 5).

Smooth-muscle bundles surrounding intrapulmonary airways showed a weak but distinct $P2X_3$ receptor labeling (as discussed later with Figures 15b and 15c). Some $P2X_3$ receptor–IR nerve fibers could be seen to loop through the bronchial smooth-muscle bundles and subsequently give rise to an intraepithelial arborization (*see* Figure 15c).

After nonamplified indirect staining using 10 μg/ml of $P2X_3$ receptor antibodies, no clear intraepithelial nerve terminals could be distinguished in rat lung; using 0.625 μg/ml there was no reaction at all. The positive control sections of vagal nodose ganglia showed a high number of $P2X_3$ receptor–IR neurons. No differences in staining patterns could be observed between the sections processed with and without TSA enhancement.

No labeled nerve endings were seen in the respiratory tract after omission of the primary or secondary antibodies from the immunocytochemical procedure. Also, preabsorption of the primary $P2X_3$ receptor antiserum with the receptor antigen abolished all staining.

Immunocytochemical Double Staining of $P2X_3$ Receptors and Neuroepithelial Bodies

Subsequent labeling of sections processed for $P2X_3$ receptor localization with antibodies to CGRP or CB (as markers for pulmonary NEB cells) showed that the intraepithelial nerve terminals in all cases coincided with the presence of an NEB (bronchial: Figures 9, 10, and 12; bronchiolar: Figures 6, 8, and 11; and alveolar: Figure 7). However, not all NEBs, marked by their CGRP or CB staining, appeared to receive a nerve ending positive for $P2X_3$ receptor immunoreactivity. Quantitative analysis (Table 1), performed to obtain more accurate data on the proportion of NEBs contacted by $P2X_3$ receptor–IR nerve terminals, revealed that about 47% of the NEBs received such a terminal, whereas 100% of the intraepithelial $P2X_3$ receptor–IR terminal arborizations coincided with the presence of NEBs.

Optical sections obtained by confocal microscopy revealed that the $P2X_3$ receptor–IR nerve fibers protrude between and surround the CGRP- or CB-positive NEB cells (Figures 6–8 and 10–12). Nerve profiles were often seen to cover the luminal surface of NEBs (Figures 7, 8, and 11), separated from the airway lumen by processes of the overlying Clara-like cells only.

Besides NEBs, CGRP immunoreactivity also labels a

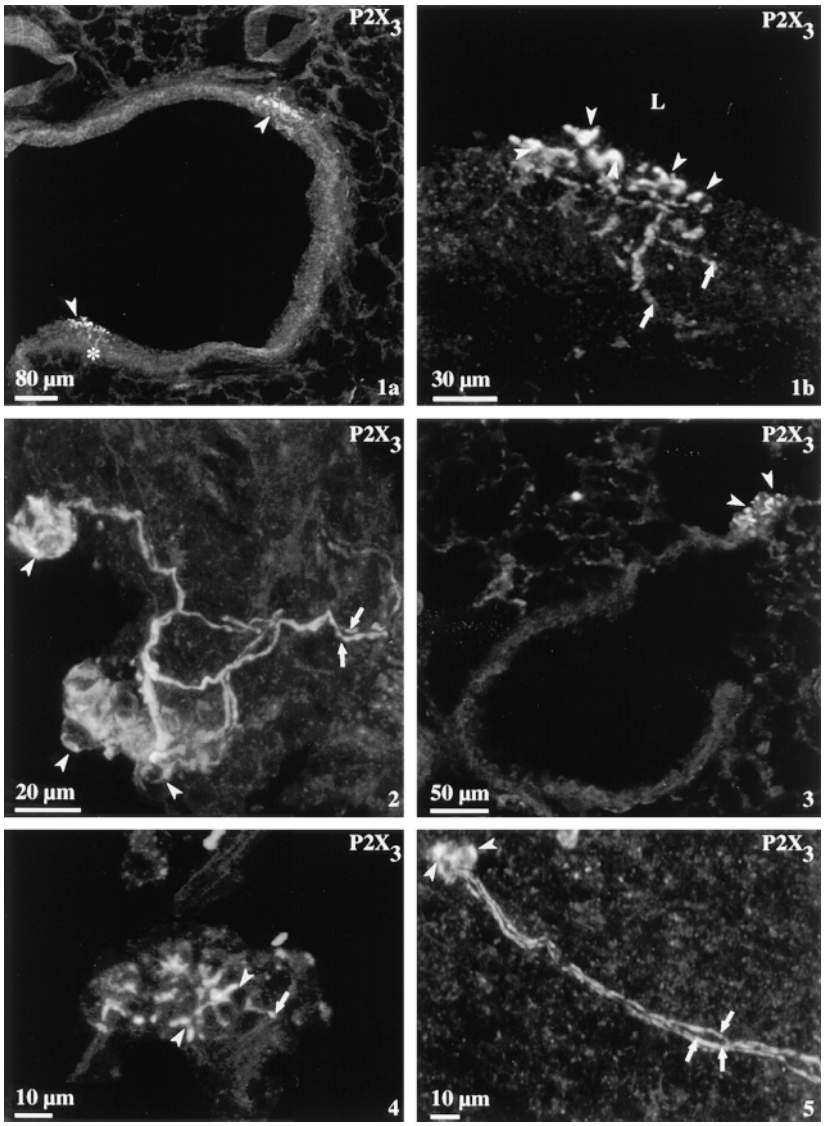

Figures 1–5 show confocal microscopic images obtained at different levels of rat intrapulmonary airways. FITC-labeled nerve fibers expressing $P2X_3$ purinoceptors (*arrows*) approach the epithelium, protrude between the epithelial cells, and from intraepithelial terminals (*arrowheads*). (Panels are labeled in lower right corners.) *Figure 1.* Branching point of an intrapulmonary bronchus. (*a*) Low-magnification overview showing two $P2X_3$ receptor–IR intraepithelial arborizations. Single optical section. (*b*) High magnification of one of the complexes (*asterisk* in *a*) shows that several nerve fibers participate in giving rise to a single intraepithelial arborization. Many terminals are seen close to the luminal surface. (L, lumen of the bronchus.) Maximum intensity projection of 20 optical sections (0.5-µm interval). *Figure 2.* Bronchiole. A network of branching $P2X_3$ receptor–IR nerve fibers gives rise to two intraepithelial terminal arborizations. Maximum intensity projection of 27 optical sections (0.95-µm interval). *Figure 3.* Terminal and respiratory bronchiole. Low-magnification overview of $P2X_3$ receptor–IR nerve terminal. Single optical section. *Figure 4.* Detail of intraepithelial $P2X_3$ receptor–IR terminals at the alveolar level. Maximum intensity projection of 12 optical sections (1-µm interval). *Figure 5.* Peripheral area. A bundle of $P2X_3$ receptor–IR nerve fibers gives rise to a single terminal complex. Maximum intensity projection of 15 optical sections (0.95-µm interval).

presumably sensory subpopulation of nerve fibers making contact with pulmonary NEBs. $P2X_3$ receptor–positive nerve endings, however, did not express CGRP immunoreactivity (Figures 6, 8, and 9).

CB immunoreactivity has recently been demonstrated to be a marker for the vagal afferent component of the innervation of NEBs (38). In cross sections of the lower trachea, $P2X_3$ receptor and CB immunoreactivity were seen in the same nerve fibers in branches of the vagal nerve. All $P2X_3$ receptor–expressing nerve fibers in contact with NEBs could subsequently be stained using antibodies to CB, although the staining intensity of both substances varied from fiber to fiber (Figures 10–12). Some CB-IR fibers, apparently not making contact with NEBs, did not express $P2X_3$ receptors.

After consecutive double labeling with two rabbit antibodies (anti-$P2X_3$ receptor and anti-CGRP or -CB, respectively) $P2X_3$ receptor immunoreactivity appeared identical to that seen in single $P2X_3$ receptor–labeled sections. No reaction was observed for the second labeling after omission of the primary antibodies.

$P2X_3$ Receptor Innervation of Quinacrine-Accumulating Neuroepithelial Bodies

At 1 d after the intraperitoneal injection of quinacrine, intraepithelial cell groups accumulating this fluorescent compound could be found at all levels of rat intrapulmonary airways (Figures 13a, 14a, and 15a). Subsequent immunocytochemical staining with antibodies to the rat NEB markers CGRP (Figure 13b) or CB (Figure 14b) revealed that the intraepithelial quinacrine-labeled cell groups invariably corresponded to pulmonary NEBs. When quinacrine loading was combined with $P2X_3$ receptor labeling, it was shown that the location of all branching intraepithelial $P2X_3$ receptor–IR nerve terminals corresponded with the presence of quinacrine-stained NEBs (Figure 15). Not all quinacrine-accumulating NEBs, however, received such nerve endings.

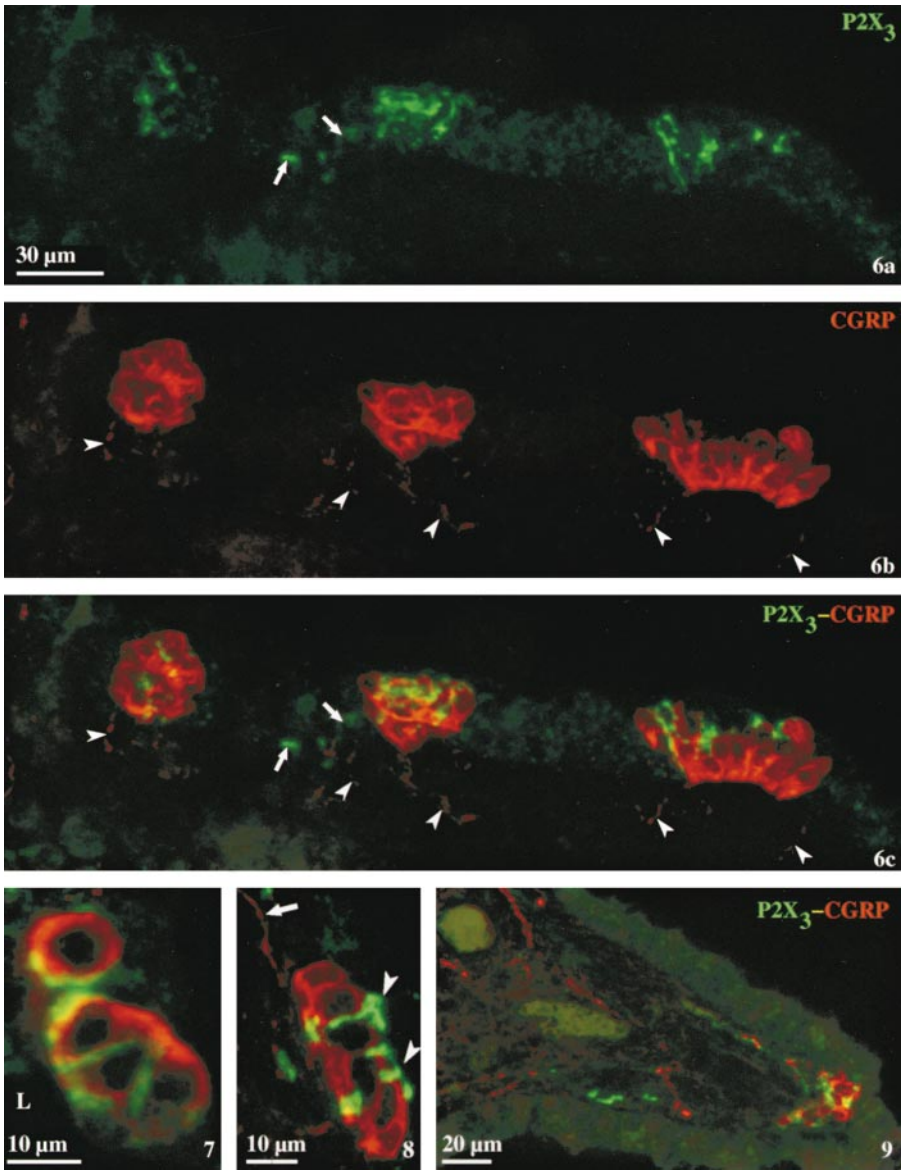

Figures 6–9 show immunocytochemical double-staining for $P2X_3$ receptors (*green* FITC fluorescence) and CGRP (*red* Cy-3 fluorescence). (Panels are labeled in lower right corners.) *Figure 6.* NEBs in a rat bronchiole are contacted by $P2X_3$ receptor–expressing and CGRP-expressing nerve fibers. Maximum intensity projections of 16 confocal optical sections (1-µm interval). (*a*) *Green* channel showing three neighboring intraepithelial complexes of $P2X_3$ receptor–IR nerve terminals. Note an approaching nerve fiber (*arrows*). (*b*) *Red* channel showing three CGRP-IR NEBs contacted by CGRP-containing nerve fibers (*arrowheads*). (*c*) Combination of both channels clearly demonstrating that $P2X_3$ receptor and CGRP immunoreactivity are located in separate nerve-fiber populations. *Figure 7.* $P2X_3$ receptor-IR nerve fibers protruding and overlying the luminal (L) surface of the CGRP-positive neuroendocrine cells of an alveolar NEB. Single confocal optical section. *Figure 8.* Single confocal optical section of a bronchiolar NEB showing $P2X_3$-IR nerve fibers protruding between the neuroendocrine cells and covering their luminal surface (*arrowheads*). Note that the CGRP-IR nerve fiber (*arrow*) contacting the NEB does not express $P2X_3$ receptors. *Figure 9.* Overview of an NEB located at a bronchial bifurcation point. $P2X_3$ receptor and CGRP staining are seen in separate nerve fiber populations. Maximum intensity projection of 19 confocal optical sections (0.95-µm interval).

Effects of Unilateral Cervical Vagal Crush on the $P2X_3$ Receptor–IR Innervation of the Rat Lower Respiratory Tract

At 3, 7, and 14 d after a unilateral cervical vagal crush, no $P2X_3$ receptor–IR nerve fibers could be observed in the lower respiratory tract of the lung ipsilateral to the denervation, whereas bronchial smooth muscle still expressed $P2X_3$ receptors. No NEBs could be observed to receive $P2X_3$ receptor–IR nerve terminals.

Lungs contralateral to the crushed side, on the other hand, did not show obvious differences in the amount or location of $P2X_3$ receptor–IR nerve fibers, as compared with control animals.

$P2X_3$ Receptor Expression in Vagal Nodose Neurons Retrogradely Traced from the Lungs

At 1 wk after instillation of Fluorogold in the lungs, the vagal sensory nodose ganglia harbored Fluorogold-traced neurons (Figure 16a), many of which were $P2X_3$ receptor–positive (Figure 16b). Just a small fraction of the $P2X_3$ receptor–expressing nodose neurons coexpressed Fluorogold, whereas only few retrogradely Fluorogold-traced neurons did not express $P2X_3$ receptors (Figure 16). The intensity of $P2X_3$ receptor staining appeared to vary from neuron to neuron (Figure 16b).

Intrapulmonary Fluorogold instillation after a unilateral cervical vagotomy resulted in the absence of Fluorogold-traced neurons in the nodose ganglion ipsilateral to the denervation side. No changes were observed in the contralateral ganglion.

Discussion

The present study describes the expression of purinergic $P2X_3$ receptors on terminal arborizations of vagal nodose afferent nerve fibers in contact with NEBs in the rat lung.

The rabbit polyclonal antibody against $P2X_3$ receptors

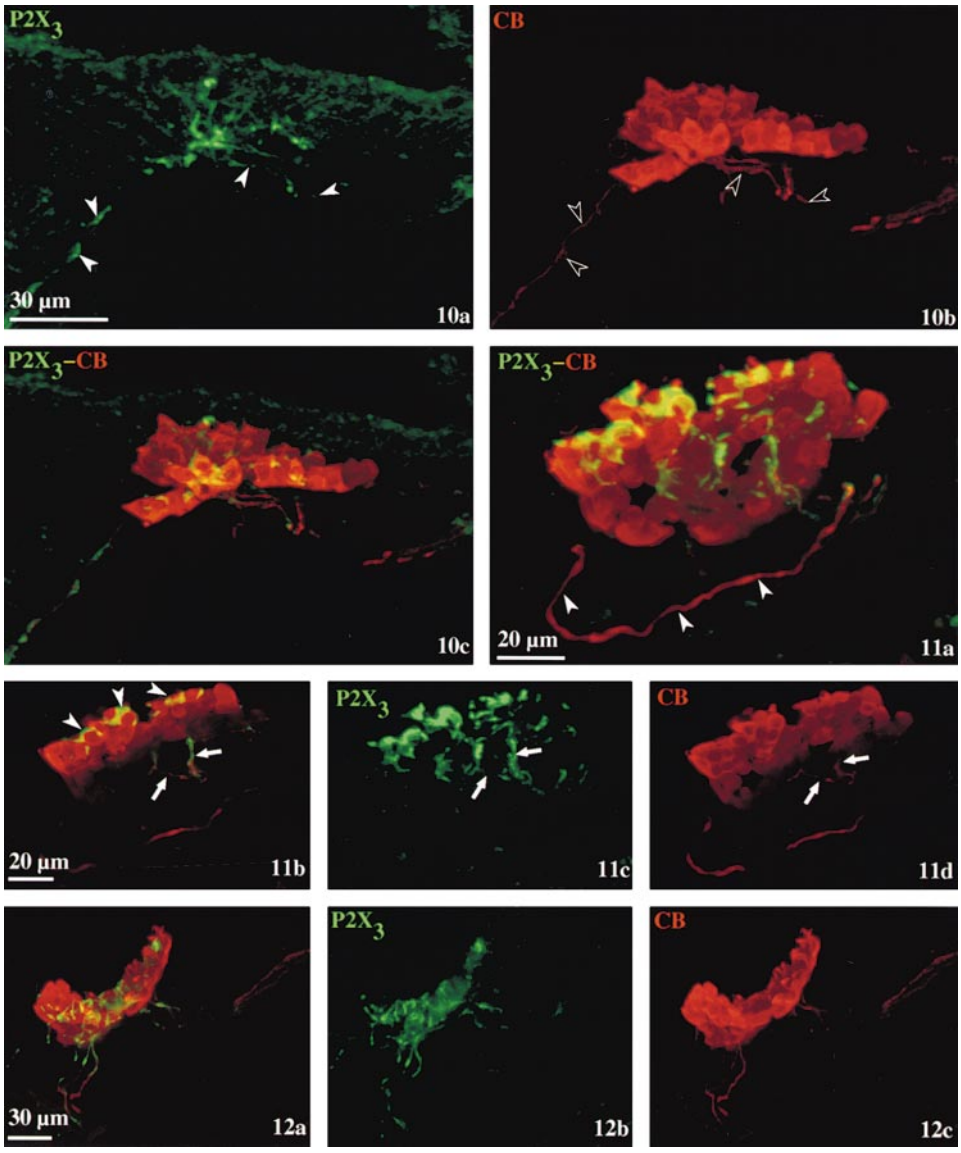

Figures 10–12 show immunocytochemical double-staining for $P2X_3$ receptors (*green* FITC fluorescence) and CB (*red* Cy-3 fluorescence). (Panels are labeled in lower right corners.) *Figure 10.* Bronchial CB-IR NEB contacted by $P2X_3$ receptor and CB-IR nerve terminals. Maximum intensity projection of 18 confocal optical sections (1-µm interval). (*a*) *Green* channel showing an intraepithelial $P2X_3$ receptor–expressing arborization originating from multiple nerve-fiber endings (*arrowheads*). (*b*) *Red* channel showing CB-IR nerve fibers (*open arrowheads*) in contact with the NEB. (*c*) Combination of both channels revealing that nerve fibers in contact with the NEB express both $P2X_3$ receptors and CB, though the staining intensity varies along the nerve fibers. *Figure 11.* Bronchiolar CB-IR NEB contacted by $P2X_3$-receptor and CB-IR nerve fibers. (*a*) Maximum intensity projection of the complete NEB and all nerve endings (eight confocal optical sections; 2-µm interval). Notice that in the lamina propria the approaching CB-IR fiber (*arrowheads*) shows no clear $P2X_3$ receptor immunoreactivity. (*b*) Reconstruction of five optical sections showing nerve fibers that colocalize $P2X_3$ receptor and CB immunoreactivity (*arrows*) enter the base of the NEB and form terminals that surround the apical region of the NEB cells (*arrowheads*). (*c*) Image identical to *a* showing the green channel only. *Arrows* point to the same fibers as in *b* and *d*. (*d*) Reconstruction of three optical sections showing the expression of CB in nerve fibers entering the NEB (*arrows*). *Figure 12.* Bronchial NEB contacted by a complex network of nerve fibers. (*a*) Combination of the green (*b*) and red (*c*) channels. A high degree of colocalization between $P2X_3$ receptor and CB immunoreactivity is obvious in the nerve fibers.

used in this study (kindly supplied by Roche Bioscience) has been characterized and found not to cross-react with other P2 receptors (29, 33). To increase the sensitivity of detection, we visualized $P2X_3$ receptor expression after amplification with biotinylated tyramide (39). We are confident that, in our results, the labeling using an indirect TSA enhancement is specific, because omission of the specific antisera or preabsorption of $P2X_3$ receptor antiserum with the receptor antigen consistently led to negative results. The necessity of TSA specifically for the clear visualization of intraepithelial nerve terminals in the rat lung in this study was demonstrated by the fact that a procedure without amplification, which gives good results in the positive control tissue, appears unable to provide a clear labeling of nerve terminals in the lung. After unilateral cervical (infranodose) vagal crush, no $P2X_3$ receptor–IR intraepithelial nerve terminals could be detected in the ipsilateral lung, arguing for the specific labeling of a subset of vagal fibers.

The use of TSA allows the consecutive application of two antisera raised in the same species, provided that the concentration of the first (enhanced) primary antibody is too low to be detectable using a nonamplified procedure (34). In the present study, the $P2X_3$ receptor staining pattern in single labeled sections was identical to that seen after double staining with CGRP. Moreover, no colocalization could be detected, clearly illustrating the absence of any cross-reaction between the antirabbit antiserum used for the visualization of rabbit anti-CGRP antibodies and the initially bound rabbit anti–$P2X_3$ receptor antibodies. A disadvantage of TSA, though, is that the diameter of IR nerve fibers often appears to be increased, most likely due to the large number of interacting proteins. This might in-

TABLE 1

Quantitative analysis of intraepithelial $P2X_3$ receptor–IR nerve terminals in rat lungs and their relation to NEBs

Number of animals included in the analysis	6
Number of sections included in the analysis	84 (14 random sections from each animal)
Total number of NEBs in the analyzed sections	393
Total number of $P2X_3$ receptor–IR intraepithelial arborizations	185
Number of $P2X_3$ receptor–IR intraepithelial arborizations colocalizing with NEBs	185
Number of $P2X_3$ receptor–IR intraepithelial nerve endings not colocalizing with NEBs	0
Percentage of the total number of NEBs that receive $P2X_3$ receptor–IR nerve endings	47.07% (185 out of 393)

fluence the interpretation of consecutive double-labeling procedures, in which some fluorescent staining appears to overlap even without being colocalized.

For $P2X_3$ receptor localization, rats of 4 to 5 wk of age were used because no difference with adult rats could be found regarding the subject of interest in this study and because the density of NEBs in relation to lung volume is higher in this age group, therefore leading to a much more efficient investigation.

The observed $P2X_3$ receptor–IR nerve fibers, protruding between the neuroendocrine cells of about 47% of the CGRP- or CB-labeled NEBs, morphologically resemble the vagal afferent component of the innervation of rat NEBs that originates in the nodose ganglia, as has been characterized in anterograde tracer experiments (8). Similar to what is seen using $P2X_3$ receptor immunoreactivity, the latter study strongly suggested that only part of the pulmonary NEBs receives a vagal nodose innervation. It was unambiguously demonstrated that NEBs receive at least two different sensory nerve fiber populations: afferent nerve fibers originating from neurons located in the nodose ganglia, of which the chemical coding needed further investigation; and putative sensory CGRP-IR fibers that do not have a vagal origin (8). Although precise information about the origin of the CGRP-IR fibers in contact with NEBs is still lacking, retrograde tracing experiments have revealed that CGRP-IR fibers in rat lungs predominantly originate from dorsal root ganglia (DRG) (40). Because $P2X_3$ receptors in rats have been localized on nerve-cell bodies in nodose ganglia as well as in DRG (24, 32), and on their central and peripheral extensions using *in situ* hybridization and immunohistochemical methods (24, 27, 29, 41, 42), theoretically both options for the origin of $P2X_3$ receptor–IR nerve fibers innervating pulmonary NEBs should be considered.

Immunohistochemical staining of sections of rat lung showed CGRP-IR nerve fibers in nerve bundles, between neurons in bronchial ganglia, between cells of the ciliomucous epithelium in large-diameter intrapulmonary and extrapulmonary bronchi, and innervating the basal pole of NEBs at all airway levels, similar to descriptions in the literature (43–45). Combination of $P2X_3$ receptor and CGRP immunohistochemistry revealed that $P2X_3$ receptor and CGRP immunoreactivity are not coexpressed in fibers contacting NEBs, indicating that different nerve fiber populations are concerned. Bradbury and colleagues (27) further showed that in DRG only few CGRP-IR perikarya also revealed $P2X_3$ receptor immunoreactivity.

After a unilateral infranodosal (cervical) vagal crush, no $P2X_3$ receptor–IR nerve fibers could be observed in the vagal nerve or surrounding NEB cells ipsilateral to the denervated side, whereas the contralateral lung appeared unchanged with regard to the distribution and morphology of $P2X_3$ receptor immunoreactivity. Because it has been shown that the vagal afferent component of the innervation of pulmonary NEBs has its origin in the ipsilateral nodose ganglia (8), these data strongly suggest that the $P2X_3$ receptor–expressing nerve terminals contacting NEBs also originate in the ipsilateral vagal nodose ganglia and that contralateral lungs may be regarded as control lungs.

Only recently, it has become clear that the calcium-binding protein CB is expressed by a subpopulation of the nerve fibers that specifically contact rat NEBs (38). It was shown that CB-positive nerve fibers innervating NEBs disappeared after infranodosal vagotomy. Therefore, CB was put forward as a marker for the vagal nodose afferent component of the innervation of rat pulmonary NEBs. TSA-enhanced $P2X_3$ receptor labeling and subsequent conventional immunocytochemical staining for CB clearly showed that $P2X_3$ receptor and CB immunoreactivity were colocalized in nerve fibers contacting NEBs. It was, however, seen that CB-IR nerve fibers approaching NEBs did not always reveal a clear $P2X_3$ receptor expression. Intraepithelially, on the other hand, $P2X_3$ receptor immunoreactivity is usually strong. This might be explained by a different expression of $P2X_3$ receptors in different regions of the neurons. Because ligand-gated ion channels are built up by receptor proteins that are synthesized in perikarya and transported to the peripheral nerve endings, accumulation of peptides and surface expression of the receptors might be higher in the peripheral nerve endings. This might explain why some pictures obtained in this study also show a difference in expression of $P2X_3$ receptors along the nerve fibers. Similarly, in single $P2X_3$ receptor–labeled sections, nerve fibers protruding between the NEB cells invariably show a bright fluorescent staining, whereas nerve fibers entering the NEB are not always clearly recognizable.

$P2X_3$ receptors were shown to be present in a subpopulation of large-, medium-, and small-sized neurons in rat nodose ganglia (24). In the present study, retrograde Fluorogold tracing from the lungs and subsequent $P2X_3$ receptor immunocytochemistry revealed that many but not all Fluorogold-labeled nodose neurons showed $P2X_3$ receptor immunoreactivity. Therefore, we may assume that different subpopulations of nodose neurons are involved in the innervation of rat lung, but only one of them gives rise to the $P2X_3$ receptor–expressing nerve terminals specifically

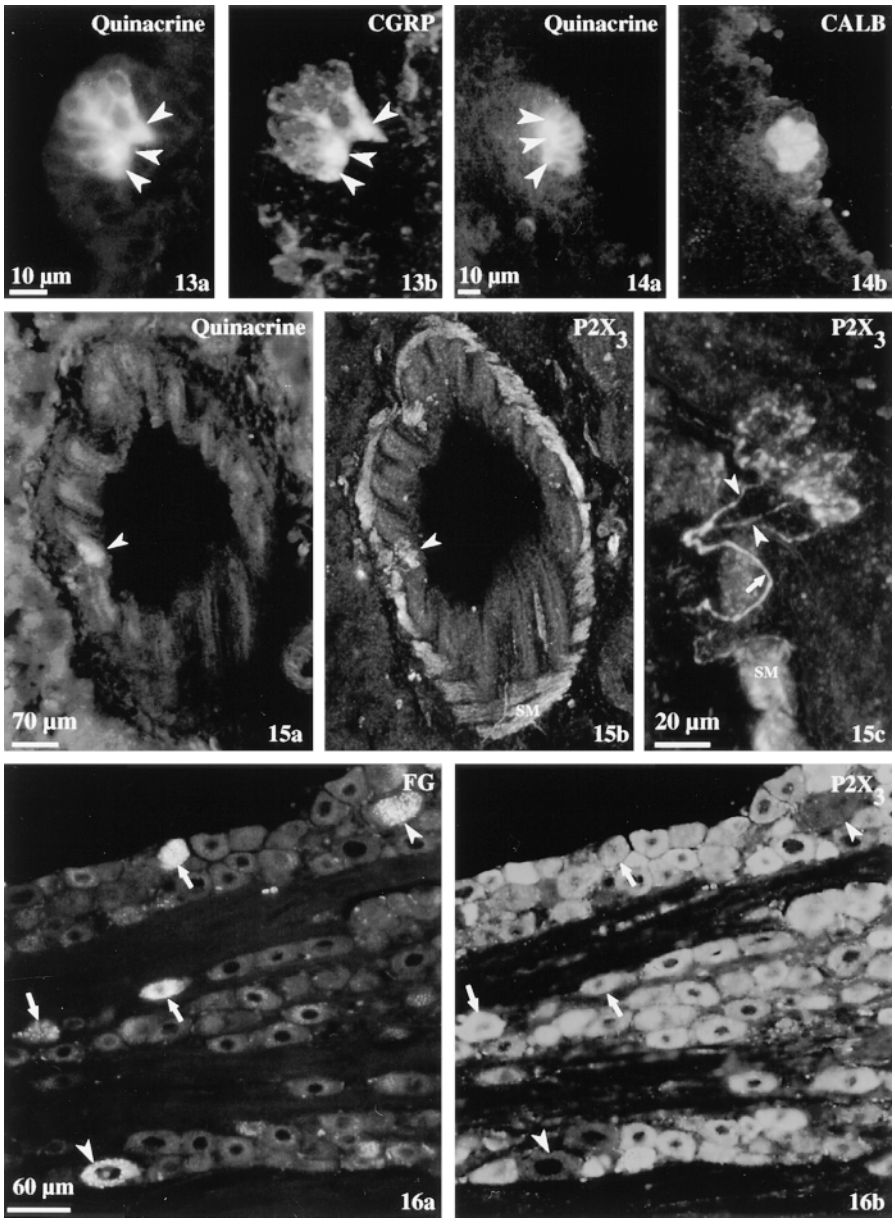

Figures 13–16. Figure 13: Quinacrine histochemistry and subsequent CGRP immunocytochemistry demonstrate that the quinacrine-accumulating intraepithelial cell group can be identified as a bronchial NEB. (*a*) Fluorescence micrograph of a quinacrine-accumulating cell group. Note that the quinacrine accumulation is most prominent at the basal pole of each individual cell (*arrowheads*). The nuclei are free of fluorescence. (*b*) The same spot as in *a* after CGRP immunostaining. Also the CGRP-immunoactivity appears to be strongest at the base of the neuroendocrine cells (*arrowheads*). The staining pattern is reminiscent of that seen in *a*. *Figure 14.* Quinacrine fluorescence (*a*) and sequential CB immunostaining (*b*) demonstrate the colocalization of quinacrine-accumulating cell groups and CB-IR NEBs. (*a*) Also in this fluorescent cell group, quinacrine accumulation is highest at the basal side (*arrowheads*). (*b*) Subsequent CB immunocytochemistry shows that CB-immunoreactivity reveals a different intracellular staining pattern. *Figure 15.* Consecutive quinacrine accumulation and $P2X_3$ receptor staining in a rat bronchus. (*a*) Fluorescence micrograph of quinacrine accumulation in an intraepithelial cell group (*arrowhead*), indicating the presence of an NEB. (*b* and *c*) $P2X_3$ receptor immunocytochemistry revealing the presence of extensive receptor-expressing nerve terminals at exactly the same spot as marked in *a* (*arrowhead*). Notice $P2X_3$ receptor-immunoreactivity in bronchial smooth muscle bundles (SM). Single confocal optical section. (*c*) High magnification detail of *b* clearly showing the $P2X_3$ receptor–IR nerve fiber (*arrow*) that loops through the smooth-muscle bundles, branches (*arrowheads*), and gives rise to a terminal intraepithelial arborization. Maximum intensity projection of 20 confocal optical sections (0.95-µm interval). *Figure 16.* Fluorescence micrographs of the nodose ganglion after consecutive retrograde tracing from rat lungs, using an intraluminal application of Fluorogold, and $P2X_3$ receptor immunolabeling. Some retrogradely Fluorogold-traced neurons (*arrows* in *a*) express $P2X_3$ receptors (*arrows* in *b*), whereas other traced neurons (*arrowheads* in *a*) do not express $P2X_3$ receptors (*arrowheads* in *b*). (*a*) Fluorogold accumulation reveals a limited number of retrogradely traced neurons. (*b*) A majority of the nodose neurons express $P2X_3$ receptors.

contacting NEBs. Because retrograde tracing after unilateral infranodosal vagotomy showed no fluorescent neurons in nodose ganglia ipsilateral to the operated side, we are confident that the fluorescent dye is transported via vagal nerve fibers and not via diffusion or the circulation. It is therefore likely that at least part of the retrogradely traced neurons expressing $P2X_3$ receptors are involved in the innervation of NEBs.

In contrast to the situation in nodose ganglia, the expression of $P2X_3$ receptors in DRG is restricted to small-sized sensory neurons that are presumed to be involved in nociceptive signaling (22, 23, 27, 46). Although the involvement of vagal afferent nerve fibers in facilitation or inhibition of nociception has been described in rats (47, 48), the preferential involvement of a specific subpopulation of nodose neurons in nociception has not yet been established.

Sensory neurons in cultured nodose ganglia demonstrated $P2X_2/P2X_3$ heteromultimeric channels, which, according to Lewis and associates (23), accounted for generation or transmission of primary afferent information. Vulchanova and coworkers (24) have shown that subpopulations of rat nodose neurons colocalize $P2X_2$ and $P2X_3$ receptor expression. Whether the $P2X_3$ receptor subunits, either alone or in combination with $P2X_2$ receptors, should

be regarded as crucial for the depolarization of the vagal fibers is not clear.

The hypothesis that $P2X_3$ receptors play a major role in nociceptive signaling gains more strength (25, 41, 49, 50). Studies using *in vivo* pain models showed that homomultimeric $P2X_3$ or heteromultimeric $P2X_2/P2X_3$ channels can be selectively stimulated by application of ATP, resulting in intense pain perception (51–53).

The most widely used method to detect an accumulation of ATP in secretory granules is quinacrine histochemistry (11, 14, 35). This antimalaria drug appears to bind to ATP (13, 54) when stored in high concentrations in secretory granules. Quinacrine histochemistry has, among others, been shown to specifically label members of the diffuse neuroendocrine system (DNES) (55), of which one of the main characteristics is the presence of dense-cored vesicles. Inasmuch as it is generally agreed that pulmonary NEBs belong to the DNES, it was not surprising that we succeeded in specifically labeling NEBs by their quinacrine accumulation (10), as was confirmed in the present study by consecutive CB or CGRP immunolabeling. Analogous with other systems, our data suggest that ATP is accumulated in the dense-cored vesicles of pulmonary NEBs.

Because ATP is able to stimulate peripheral nociceptors, resulting in intense pain and increased sensory discharge (51), we suggest that release of ATP by NEB cells as a reaction to a specific stimulus might result in pain perception via a vagal afferent mechanism. Therefore, pulmonary NEBs could be added to the list of possible sources of ATP acting on $P2X_3$ receptors in relation to pain (31, 49).

NEBs are well placed to perform chemoreceptor functions (7, 8). A carotid body–like oxygen-sensing mechanism has been identified on the surface membrane of NEB cells (5, 6). In several species, subpopulations of NEBs appear to be "closed," buried in the epithelium and without direct contact with the airway lumen. The possibility that some NEBs might act as mechanoreceptors has never been ruled out (56–59), but no direct evidence could be presented. Recently, Burnstock (60) has proposed that in hollow organs and tubes, the pain caused by distension works through a purinergic mechanosensory transduction mechanism. Although the presence of other P2X receptors in lungs is still under investigation, the present study unmasks NEBs as sources of secretable ATP, potentially involved in nociception via contacting $P2X_3$ receptor–expressing vagal sensory nerve terminals.

Taking into account that in many organs ATP is believed to mediate activities in health and disease (for review, *see* Reference 61), the interaction between NEBs and $P2X_3$ receptor–IR vagal afferents may just be the first of several purinergic signaling pathways to be morphologically characterized in lungs. Inasmuch as only a subpopulation (ca. 47%) of ATP-storing NEBs appears to receive $P2X_3$ receptor–expressing nerve terminals, it will be interesting to investigate the presence of other P2 receptor subtypes as well.

In conclusion, the expression of purinergic $P2X_3$ receptors on terminal arborizations of vagal nodose afferent nerve fibers contacting pulmonary NEBs indicates that purines, or more specifically ATP, may have direct actions in the local control of rat lungs. The intimate relationship between intrapulmonary vagal afferent nerve terminals expressing $P2X_3$ receptors and ATP-storing NEB cells may represent the morphologic substrate for the vagal afferent ATP-mediated transmission that has been postulated in the literature. Whether the involved vagal nodose neurons, expressing $P2X_3$ receptors on their cell bodies and peripheral extensions, indeed belong to nociceptive signaling pathways is of great medical interest and will need further investigation.

Acknowledgments: This study was supported by an IWT grant (SB 981363 to I.B.) from the Flemish government. The authors thank M. Bardini (Autonomic Neuroscience Institute) for technical assistance, and D. De Rijck and J. Van Daele for help with the illustrations.

References

1. Scheuermann, D. W. 1987. Morphology and cytochemistry of the endocrine epithelial system in the lung. *Int. Rev. Cytol.* 106:35–88.
2. Sorokin, S. P., and R. F. Hoyt. 1989. Neuroepithelial bodies and solitary small-granule cells. *In* Lung Cell Biology. D. Massaro, editor. Marcel Dekker, New York. 191–344.
3. Adriaensen, D., and D. W. Scheuermann. 1993. Neuroendocrine cells and nerves of the lung. *Anat. Rec.* 236:70–85.
4. Lauweryns, J. M., and A. Van Lommel. 1986. Effect of various vagotomy procedures on the reaction to hypoxia of rabbit neuroepithelial bodies: modulation by intrapulmonary axon reflexes. *Exp. Lung. Res.* 11:319–339.
5. Youngson, C. R., C. Nurse, H. Yeger, and E. Cutz. 1993. Oxygen sensing in airway chemoreceptors. *Nature* 365:153–155.
6. Youngson, C. R., C. Nurse, H. Yeger, J. T. Curnutte, C. Vollmer, V. Wong, and E. Cutz. 1997. Immunocytochemical localization on O_2-sensing protein (NADPH oxidase) in chemoreceptor cells. *Microsc. Res. Tech.* 37: 101–106.
7. Sorokin, S. P., and R. F. Hoyt. 1990. On the supposed function of neuroepithelial bodies in adult mammalian lungs. *News Physiol. Sci.* 5:89–95.
8. Adriaensen, D., J.-P. Timmermans, I. Brouns, H.-R. Berthoud, W. L. Neuhuber, and D. W. Scheuermann. 1998. Pulmonary intraepithelial vagal nodose afferent nerve terminals are confined to neuroepithelial bodies: an anterograde tracing and confocal microscopy study in adult rats. *Cell Tissue Res.* 293:395–405.
9. Van Lommel, A., J. M. Lauweryns, and H.-R. Berthoud. 1998. Pulmonary neuroepithelial bodies are innervated by vagal afferent nerves: an investigation with in vivo anterograde DiI tracing and confocal microscopy. *Anat. Embryol.* 197:325–330.
10. Brouns, I., D. Adriaensen, D. W. Scheuermann, and J.-P. Timmermans. 1999. Identification of pulmonary neuroepithelial bodies by fluorescent histochemical labelling with quinacrine. *Ann. Anat.* 181:86–87. (Abstr.)
11. Crowe, R., and G. Burnstock. 1981. Comparative studies of quinacrine-positive neurones in the myenteric plexus of stomach and intestine of guinea-pig, rabbit and rat. *Cell Tissue Res.* 221:93–107.
12. Crowe, R., and G. Burnstock. 1982. Fluorescent histochemical localisation of quinacrine-positive neurones in the guinea-pig and rabbit atrium. *Cardiovasc. Res.* 16:384–390.
13. Irvin, J. L., and E. M. Irvin. 1954. The interaction of quinacrine with adenine nucleotides. *J. Biol. Chem.* 210:45–56.
14. Olson, L., M. Ålund, and K.-A. Norberg. 1976. Fluorescence microscopical demonstration of a population of gastro-intestinal nerve fibres with a selective affinity for quinacrine. *Cell Tissue Res.* 171:407–423.
15. Burnstock, G. 1996. Development and perspectives of the purinoceptor concept. *J. Auton. Pharmacol.* 16:295–302.
16. Burnstock, G. 1978. A basis for distinguishing two types of purinergic receptor. *In* Cell Membrane Receptors for Drugs and Hormones: A Multidisciplinary Approach. R. W. Straub and L. Bolis, editors. Raven Press, New York. 107–118.
17. Abbracchio, M. P., and G. Burnstock. 1994. Purinoceptors: are there families of P2X and P2Y purinoceptors? *Pharmacol. Ther.* 64:445–475.
18. Burnstock, G., and C. Kennedy. 1985. Is there a basis for distinguishing two types of P2-purinoceptor? *Gen. Pharmacol.* 16:433–440.
19. Burnstock, G., and B. F. King. 1996. Numbering of cloned P2 purinoceptors. *Drug Dev. Res.* 8:67–71.
20. Collo, G., R. A. North, E. Kawaskima, E. Merlo-Pich, S. Neidhart, A. Surprenant, and G. Buell. 1996. Cloning of $P2X_5$ and $P2X_6$ receptors and the distribution and properties of an extended family of ATP-gated ion channels. *J. Neurosci.* 16:2495–2507.
21. Burnstock, G. 1997. The past, present and future of purine nucleotides as signalling molecules. *Neuropharmacology* 36:1127–1139.
22. Chen, C.-C., A. N. Akoplan, L. Sivilotti, D. Colquhoun, G. Burnstock, and J. N. Wood. 1995. A P2X purinoceptor expressed by a subset of sensory neurons. *Nature* 377:428–431.

23. Lewis, C., S. Nelhardt, C. Holy, R. A. North, G. Buell, and A. Surprenant. 1995. Coexpression of $P2X_2$ and $P2X_3$ receptor subunits can account for ATP-gated currents in sensory neurons. *Nature* 377:432–435.
24. Vulchanova, L., M. S. Riedl, S. J. Shuster, G. Buell, A. Surprenant, R. A. North, and R. Elde. 1997. Immunohistochemical study of the $P2X_2$ and $P2X_3$ receptor subunits in rat and monkey sensory neurons and their central terminals. *Neuropharmacology* 36:1229–1242.
25. Cook, S. P., L. Vulchanova, K. M. Hargreaves, R. Elde, and E. W. McCleskey. 1997. Distinct ATP receptors on pain-sensing and stretch–sensing neurons. *Nature* 387:505–508.
26. Garcia-Guzman, M., W. Stuhmer, and F. Soto. 1997. Molecular characterization and pharmacological properties of the human $P2X_3$ purinoceptor. *Mol. Brain Res.* 47:59–66.
27. Bradbury, E. J., G. Burnstock, and S. B. McMahon. 1998. The expression of $P2X_3$ purinoreceptors in sensory neurons: effects of axotomy and glial-derived neurotrophic factor. *Mol. Cell. Neurosci.* 12:256–268.
28. Bo, X., A. Alavi, Z. Xiang, I. Oglesby, A. Ford, and G. Burnstock. 1999. Localization of ATP-gated $P2X_2$ and $P2X_3$ receptor immunoreactive nerves in rat taste buds. *Neuroreport* 10:1107–1111.
29. Llewellyn-Smith, I. J., and G. Burnstock. 1998. Ultrastructural localization of $P2X_3$ receptors in rat sensory neurons. *Neuroreport* 9:2545–2550.
30. Burnstock, G., and J. N. Wood. 1996. Purinergic receptors: their role in nociception and primary afferent neurotransmission. *Curr. Opin. Neurobiol.* 6:526–532.
31. Burnstock, G. 2000. P2X receptors in sensory neurones. *Br. J. Anaesth.* 84:476–488.
32. Xiang, Z., X. Bo, and G. Burnstock. 1998. Localization of ATP-gated P2X receptor immunoreactivity in rat sensory and sympathetic ganglia. *Neurosci. Lett.* 256:105–108.
33. Oglesby, I. B., W. G. Lachnit, G. Burnstock, and A. P. D. W. Ford. 1999. Subunit specificity of polyclonal antisera to the carboxy terminal regions of P2X receptors, $P2X_1$ through $P2X_7$. *Drug Dev. Res.* 47:189–195.
34. Michael, G. J., S. A. Averill, A. Nitkunan, M. Rattray, D. L. H. Bennett, Q. Yan, and J. V. Priestley. 1997. Nerve growth factor treatment increases brain-derived neurotrophic factor selectively in trkA-expressing dorsal root ganglion cells and in their central terminators within the spinal cord. *J. Neurosci.* 17:8476–8490.
35. Ekelund, M., B. Ahren, R. Håkanson, I. Lundquist, and F. Sundler. 1980. Quinacrine accumulates in certain peptide hormone-producing cells. *Histochemistry* 66:1–9.
36. Kummer, W., A. Fischer, R. Kurkowski, and C. Heym. 1992. The sensory and sympathetic innervation of guinea pig lung and trachea as studied by retrograde neuronal tracing and double-labelling immunohistochemistry. *Neuroscience* 49:715–737.
37. Schmued, L. C., and J. H. Fallon. 1986. Fluoro-gold: a new fluorescent retrograde axonal tracer with numerous unique properties. *Brain Res.* 377: 147–154.
38. Adriaensen, D., M. Gajda, I. Brouns, D. W. Scheuermann, and J.-P. Timmermans. 1999. Calbindin D28k is a marker for pulmonary neuroepithelial bodies and for the vagal sensory component of their innervation in rats. *FASEB J.* 13:A822. (Abstr.)
39. King, G., S. Payne, F. Walker, and G. I. Murray. 1997. A highly sensitive detection method for immunohistochemistry using biotinylated tyramine. *J. Pathol.* 183:237–241.
40. Springall, D. R., A. Cadieux, H. Oliveira, H. Su, D. Rayston, and J. M. Polak. 1987. Retrograde tracing shows that CGRP-immunoreactive nerves of rat trachea and lung originate from vagal and dorsal root ganglia. *J. Auton. Nerv. Syst.* 20:155–166.
41. Kennedy, C., and P. Leff. 1995. Painful connection for ATP. *Nature* 377: 385–386.
42. Vulchanova, L., U. Arvidsson, M. S. Riedl, J. Wang, G. Buell, A. Surprenant, R. A. North, and R. Elde. 1996. Differential distribution of two ATP-gated channels (P2X receptors) determined by immunocytochemistry. *Proc. Natl. Acad. Sci. USA* 93:8063–8067.
43. Sorokin, S. P., R. F. Hoyt, and M. J. Shaffer. 1997. Ontogeny of neuroepithelial bodies: correlations with mitogenesis and innervation. *Microsc. Res. Tech.* 37:43–61.
44. Terada, M., T. Iwanaga, H. Takahashi-Iwanaga, I. Adachi, M. Arakawa, and T. Fujita. 1992. Calcitonin gene-related peptide (CGRP)-immunoreactive nerves in the tracheal epithelium of rats: an immunohistochemical study by means of whole mount preparations. *Arch. Histol. Cytol.* 55:219–233.
45. Cadieux, A., D. R. Springall, P. K. Mulderry, J. Rodrigo, M. A. Ghatei, G. Terenghi, S. R. Bloom, and J. M. Polak. 1986. Occurrence, distribution and ontogeny of CGRP immunoreactivity in the rat lower respiratory tract: effect of capsaicin treatment and surgical denervations. *Neuroscience* 19:605–627.
46. Novakovic, S. J., L. C. Kassotakis, I. B. Oglesby, J. A. M. Smith, R. M. Eeglen, A. P. D. W. Ford, and J. C. Hunter. 1999. Immunocytochemical localization of $P2X_3$ purinoceptors in sensory neurons in naive rats and following neuropathic injury. *Pain* 80:273–282.
47. Randich, A., and G. F. Gebhart. 1992. Vagal afferent modulation of nociception. *Brain Res. Brain Res. Rev.* 17:77–99.
48. Ren, K., M. Zhuo, A. Randich, and G. F. Gebhart. 1993. Vagal afferent stimulation-produced effects on nociception in capsaicin-treated rats. *J. Neurophysiol.* 69:1530–1540.
49. Burnstock, G. 1996. A unifying purinergic hypothesis for the initiation of pain. *Lancet* 347:1604–1605.
50. Evans, R. J., and A. Surprenant. 1996. P2X receptors in autonomic and sensory neurons. *Semin. Neurosci.* 8:217–223.
51. Bland-Ward, P. A., and P. P. A. Humphrey. 1997. Acute nociception mediated by hindpaw P2X receptor activation in the rat. *Br. J. Pharmacol.* 122:365–371.
52. Dowd, E., D. S. McQueen, I. P. Chessell, and P. P. A. Humphrey. 1998. P2X receptor-mediated excitation of nociceptive afferents in the normal and arthritic rat knee joint. *Br. J. Pharmacol.* 125:341–346.
53. Trezise, D. J., and P. P. A. Humphrey. 1997. Activation of cutaneous afferent neurones by ATP. *In* Experimental Headache Models, Frontiers in Headache Research. S. P. Olesen and M. A. Moscowitz, editors. Raven Press, New York. 111–116.
54. Da Prada, M., J. G. Richards, and H. P. Lorez. 1978. Blood platelets and biogenic monoamines: biochemical, pharmacological, and morphological studies. *In* Platelets: A Multidisciplinary Approach. G. de Gaetano and S. Garattini, editors. Raven Press, New York. 331–353.
55. Böck, P. 1980. Identification of paraneurons by labelling with Quinacrine (Atebrin). *Arch. Histol. Jpn.* 43:35–44.
56. Lauweryns, J. M., M. Cokelaere, and P. Theunynck. 1972. Neuroepithelial bodies in the respiratory mucosa of various mammals: a light optical, histochemical and ultrastuctural investigation. *Z. Zellforsch. Mikrosk. Anat.* 135:569–592.
57. Lauweryns, J. M., J. C. Peuskens. 1972. Neuroepithelial bodies (neuroreceptor or secretory organs?) in human infant bronchial epithelium. *Anat. Rec.* 172:471–482.
58. Lauweryns, J. M., M. Cokelaere, and P. Theunynck. 1973. Serotonin producing neuroepithelial bodies in rabbit respiratory mucosa. *Science* 180: 410–413.
59. Wasano, K., and T. Yamamoto. 1978. Monoamine-containing granulated cells in the frog lung. *Cell Tissue Res.* 193:201–209.
60. Burnstock, G. 1999. Release of vasoactive substances from endothelial cells by shear stress and purinergic mechano-sensory transduction. *J. Anat.* 194: 335–343.
61. Abbracchio, M., and G. Burnstock. 1998. Purinergic signalling: pathophysiological roles. *Jpn. J. Pharmacol.* 78:113–145.